

Supporting Information
RCA-Assisted CRISPR/Cas9 Cleavage (RACE) for Highly Specific Detection of
Multiple Extracellular Vesicle MicroRNAs

Ruixuan Wang^{1,2,3*}, Xianxian Zhao^{3*}, Xiaohui Chen^{2,4}, Xiaopei Qiu^{2,3}, Guangchao Qing^{2,4}, Hong Zhang^{2,4}, Liangliang Zhang^{2,4}, Xiaolin Hu^{2,4}, Zhuoqi He⁴, Daidi Zhong⁴, Ying Wang⁵, Yang Luo^{2,4†}

¹School of Materials and Energy, Southwest University, Tiansheng Street, Beibei, Chongqing, 400715, China.

²Center of Smart Laboratory and Molecular Medicine, Medical School, Chongqing University, Chongqing, 400044, China.

³Department of Clinical Laboratory Medicine, Southwest Hospital, Army Medical University, Chongqing, 400038, China.

⁴Key Laboratory for Biorheological Science and Technology of Ministry of Education, State and Local Joint Engineering Laboratory for Vascular Implants, Bioengineering College of Chongqing University, Chongqing, 400044, China.

⁵Department of Laboratory Medicine, Chongqing University Cancer Hospital and Chongqing Cancer Institute and Chongqing Cancer Hospital, 400030, China.

*These authors contributed equally to this work.

†Send correspondence to: luoy@cqu.edu.cn.

This material includes:

Table S1. Sequences of DNA oligonucleotides used in this work.

Table S2. Sequences of sgRNAs and Cas9.

Table S3. Sequences of primer in RT-qPCR.

Table S4. EV-derived microRNAs detection methods.

Figure S1. Expression and purification of the Cas9 proteins.

Figure S2. PAGE electrophoresis profiles.

Figure S3. The ssDNA amplicon reached a length of $\sim 10^4$ nt within 2 h.

Figure S4. The electrophoresis profile of miR-21 detection after CRISPR/Cas9 cleavage.

Figure S5. PAGE electrophoresis analysis of miR-221 detection.

Figure S6. The FI of concentration change and the calibration curve of miRNA-221.

Figure S7. The FI of concentration change and the calibration curve of miRNA-222.

Figure S8. Representative interference experiments for miR-21 (50 nM) detection.

Figure S9. Cellular miR-21 determined by RT-qPCR.

Figure S10. Methodological comparison between RT-qPCR and RACE in detecting miR-221.

Figure S11. Methodological comparison between RT-qPCR and RACE in detecting miR-222.

Figure S12. TEM image of the isolated extracellular vesicles from plasma.

Figure S13. Plasma EV-derived miR-221 was detected between healthy individuals and NSCLCs patients.

Figure S14. Plasma EV-derived miR-222 was detected between healthy individuals and NSCLCs patients.

Figure S15. The PAGE electrophoresis analysis of multiple interferences.

Table S1. Sequences of DNA oligonucleotides used in this work.

Name	Sequences
PP1(PP-21)	5'-TGACTACAAC TAGGAAAGGGGGGAAGGGGGTGGAAAAGGGGAGATCGAATAGTC-3'
PP2	5'-TGACTACAAC TAGGAAAAAAAAAAAAAGGGGTGGAAAAGGGGAGATCGAATAGTC-3'
PP3	5'-TGACTACAAC TAGGTTATTTTTTTTTTTTTTTGGTTTTGGGCAGATCGAATAGTC-3'
PP4	5'-TGACTACAAC TAGGAAACCCCCCCCCCCCCCTGGAAAACCCAGATCGAATAGTC-3'
PP-221	5'-GACGACCCAAAGAGGAAAGGGGGGAAGGGGGTGGAAAAGGGGAGTCGATGTAACA -3'
PP-222	5'-CGATGACCCAAGGAAAGGGGGGAAGGGGGTGGAAAAGGGGAGTCGATGTAGAC -3'
miR-21	5'UAG CUU AUC AGA CUG AUG UUG A 3'
Mis-1	5'UAG CUU AUC AUA CUG AUG UUG A 3'
Mis-2	5'UAG CUU AUC AUC CUG AUG UUG A 3'
Mis-3	5'UAG CUU AUC AUC GUG AUG UUG A 3'
miR-221	5'AGC UAC AUU GUC UGC UGG GUU UC 3'
miR-222	5'AGC UAC AUC UGG CUA CUG GGU 3'
TP-21	5' FAM-GGATCAACATCAGTCTGATAAGCTAGA-BHQ-1 3'
TP-221	5' Cy3-GGAGAAACCCAGCAGACAATGTAGCTGA-BHQ-2 3'
TP-222	5' Cy5-GGAACCCAGTAGCCAGATGTAGCTGA-BHQ-2 3'

Table S2. Sequences of sgRNAs and Cas9.

Name	Sequences
sgRNA-21	CGAATAGTCTGACTACAACTgttttagagctagaaatagcaagttaaataaggctagtcggttatcaactgaaaaagggcaccgagtcggtgct
sgRNA-221	ATGTAACAGACGACCCAAAGgttttagagctagaaatagcaagttaaataaggctagtcggttatcaactgaaaaagggcaccgagtcggtgct
sgRNA-222	CGATGTAGACCGATGACCCAgttttagagctagaaatagcaagttaaataaggctagtcggttatcaactgaaaaagggcaccgagtcggtgct
Cas9	<p> DKKYSIGLAIGTNSVGWAVITDEYKVPSSKKFKVLGNTDRHSIKKNLIGALLFDSGETAEATRLKRTARRRY TRRKNRICYLQEIFSNEMAKVDDSFHRLSEESFLVEEDKKHERHPIFGNIVDEVAYHEKYPTIYHLRKKLVD STDKADLRLLIYLALAHMIKFRGHFLIEGDLNPDNSVDKLFQQLVQTYNQLFEENPINASGVDAKAILSARL SKSRRLLENLIAQLPGEKKNGLFGNLIALSLGLTPNFKSNFDLAEDAKLQLSKDTYDDDLNLLAQIGDQYA DLFLAAKNLSDAILLSDILRVNTEITKAPLSASMIKRYDEHHQDLTLLKALVRQQLPEKYKEIFFDQSKNGY AGYIDGGASQEEFYKFIKPILEKMDGTEELLVKLNREDLLRKQRTFDNGSIPHQIHLGELHAILRRQEDFYPF LKDNREKIEKILTFRLPYVVGPLARGNSRFAWMTRKSEETITPWNFEVVVDKGASQSFIERMTNFDKNLP NEKVLPHKSLLEYEFTVYNELTKVKYVTEGMRKPAFLSGEQKKAIVDLLFKTNRKVTVKQLKEDYFKKIE CFDSVEISGVEDRFNASLGTYHDLLKIIKDKDFLDNEENEDILEDIVLTLTLFEDREMIERLKYAHLFDDK VMKQLKRRRYTGWGRLSRKLINGIRDKQSGKTILDFLKSDFANRNFQMQLIHDDSLTFKEDIQKAQVSGQ GDLSLHEHIANLAGSPAIAKKGILQTVKVVDELVKVMGRHKPENIVIAMARENQTTQKGQKNSRERMKRIEE GIKELGSQILKEHPVENTQLQNEKLYLYLQNGRDMYVDQELDINRLSDYDVDAIVPQSFLKDDSIDNKVL TRSDKNRGKSDNVPSEEVVKKMKNYWRQLLNAKLITQRKFDNLTKAERGGSELKAGFIKRQLVETRQI TKHVAQILDSRMNTKYDENDKLIREVKVITLKSCLVSDFRKDFQFYKVRINNYHHAHDAYLNAVVGTA IKKYPKLESEFVYGDYKVYDVRKMIKSEQEIGKATAKYFFYSNIMNFFKTEITLANGEIRKRPLIETNGET GEIVWDKGRDFATVRKVLSPQVNIVKKTEVQTGGFSKESILPKRNSDKLIARKKDWDPKKYGGFDSPTV AYSVLVVAKEVGKSKKLKSVKELLGITIMERSSEFKNPIDFLEAKGYKEVKKDLIIKLPKYSLELENGRK RMLASAGELQKGNELALPSKYVNFLYLASHYEKLGKSPEDNEQQLFVEQHKHYLDEIIEQISEFSKRVL DANLDKVLSAYNKHRDKPIREQAENIIHLFTLTNLGAPAAFKYFDTTIDRKRYTSTKEVLDTLIHQSI YETRIDLSQLGGDLEHHHHHH </p>

Table S3. Sequences of primer in RT-qPCR.

Primer	Sequences
RT-PCR	
miR-21	CTCGTATCCAGTGCAGGGTCCGAGGTATTCGCACTGGATACGAGTCAACA
miR-221	CTCGTATCCAGTGCAGGGTCCGAGGTATTCGCACTGGATACGAGGAAACC
miR-222	CTCGTATCCAGTGCAGGGTCCGAGGTATTCGCACTGGATACGAGACCCAG
qPCR	
miR-21	F: cgcgcgcgTAGCTTATCAGACTGA R: ATCCAGTGCAGGGTCCGAGG
miR-221	F: cgcgcgcgAGCTACATTGTCTGCT R: ATCCAGTGCAGGGTCCGAGG
miR-222	F: cgcgcgcgAGCTACATCTGGCTAC R: ATCCAGTGCAGGGTCCGAGG
U6	F: GGTCGGGCAGGAAAGAGGGC R: GCTAATCTTCTCTGTATCGTTCC

Table S4. EV-derived miRNAs detection methods comparison.

miRNAs Detection Methods	Temperature	Detection site	Detection target	Sensitivity	Single-base specificity	Ref
Northern Blot	Room temperature	Extracellular	Multiple targets	0.7 µg/µL	–	1
RT-qPCR	Variable temperature (4~95 °C)	Extracellular	One target	1~10 aM	–	2
SplintR-qPCR	Variable temperature (4~95 °C)	Extracellular	One target	100 aM	–	2
miREIA	Room temperature	Extracellular	One target	10 aM	–	2
Molecular Beacon	Room temperature	<i>In situ</i>	Multiple targets	100 pM	–	3,4
This method	Room temperature	Extracellular	Multiple targets	90 fM	+	

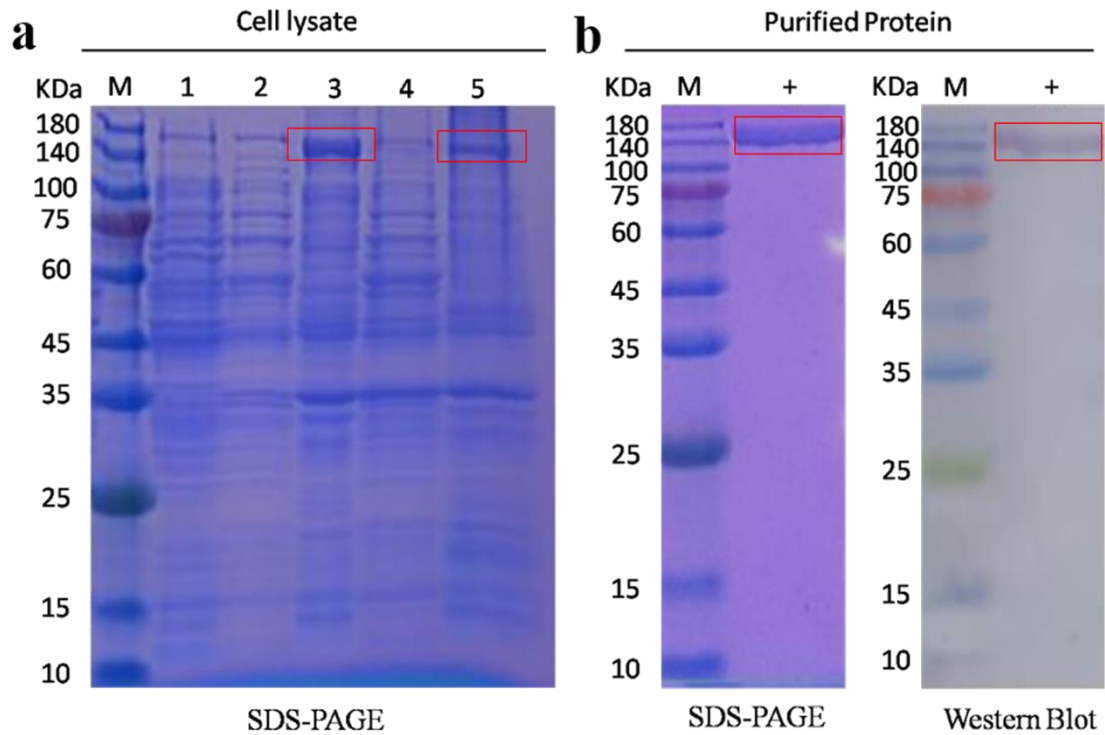


Figure S1. Expression and purification of the Cas9 proteins. **a** SDS-PAGE analysis of cell lysate. M: Prestained Marke, 1: Total protein before induction, 2: Cell supernatant in 20°C, 3: Cell precipitate in 20°C, 4: Cell supernatant in 37°C, 5: Cell precipitate in 37°C. **b** SDS-PAGE and western blot analysis of Cas9 with 159.2 KD. M: Prestained Marke, +: Purified Cas9.

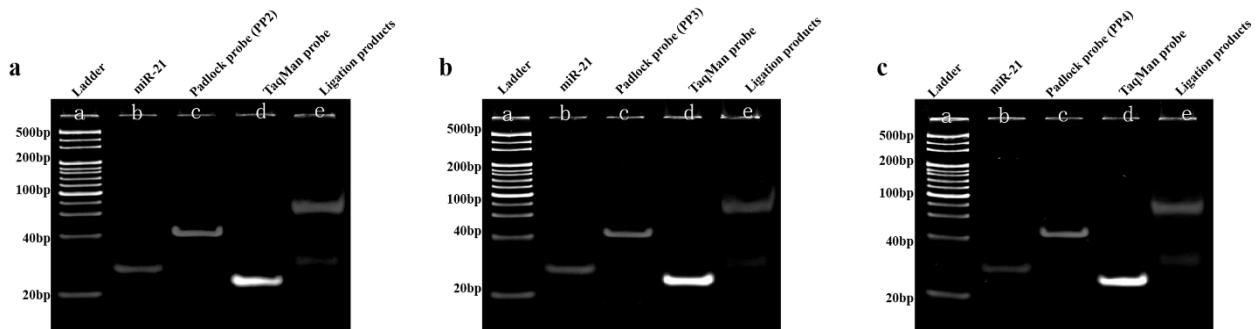


Figure S2. PAGE electrophoresis profiles. **a** ladder (lane a), miR-21 (lane b), PP2 (lane c), Ligation products (lane d), RCA products (lane e). **b** ladder (lane a), miR-21 (lane b), PP3 (lane c), Ligation products (lane d), RCA products (lane e). **c** ladder (lane a), miR-21 (lane b), PP4 (lane c), Ligation products (lane d), RCA products (lane e).

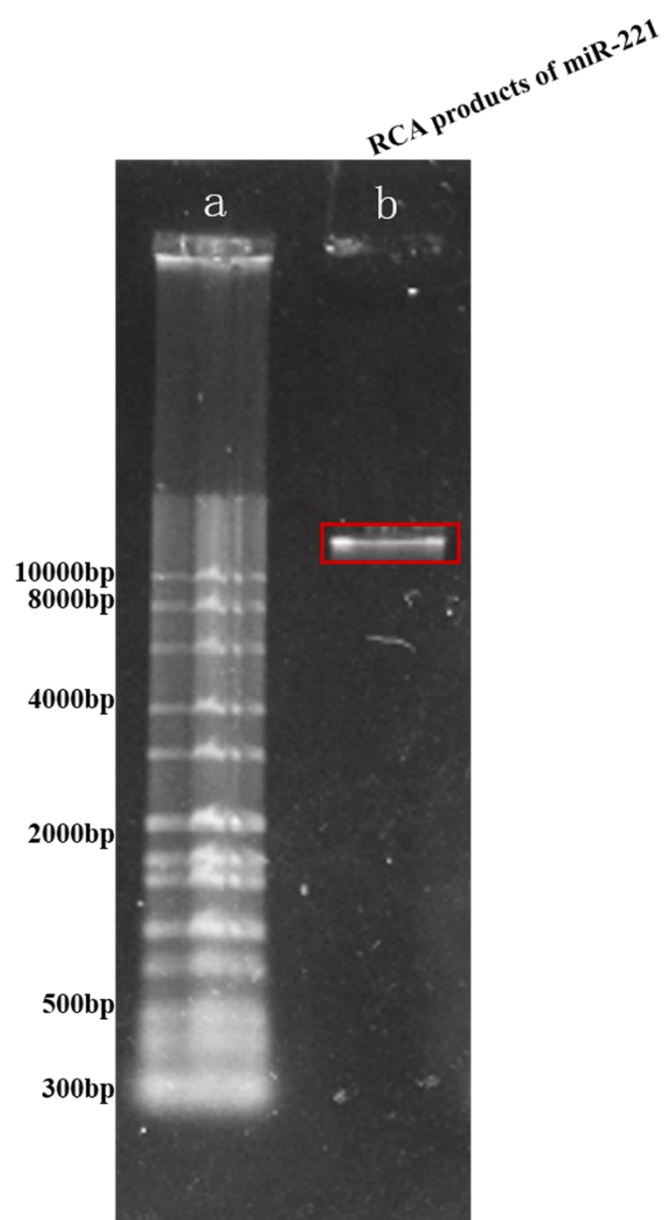


Figure S3. The ssDNA amplicon reached a length of $\sim 10^4$ nt within 2 h.

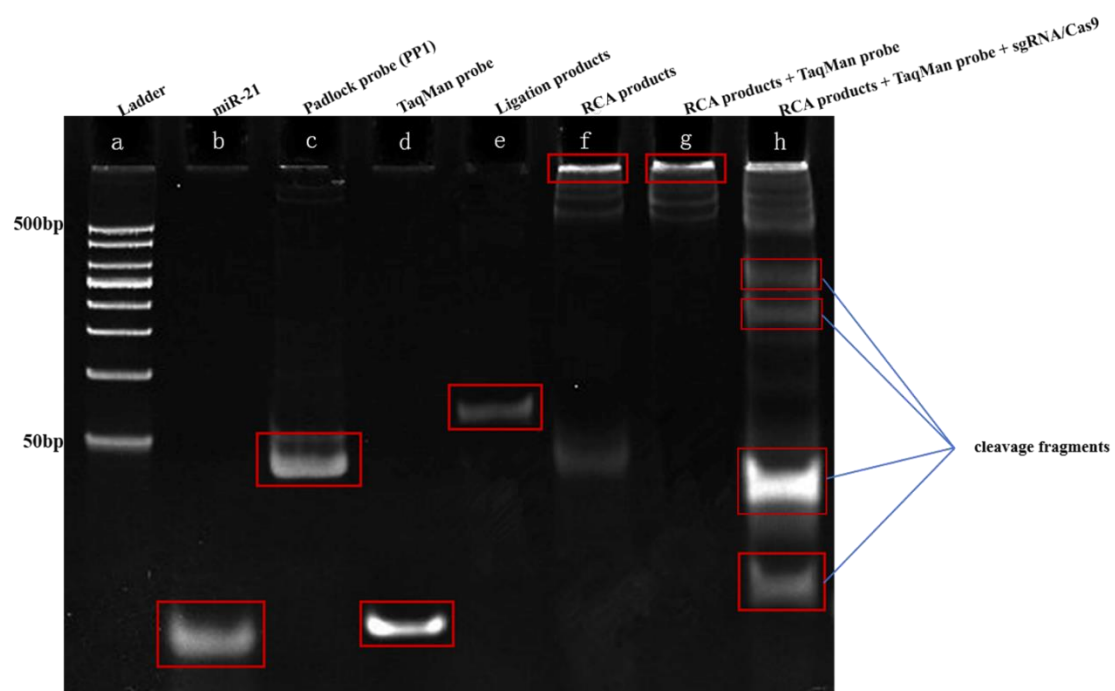


Figure S4. The electrophoresis profile of miR-21 detection after CRISPR/Cas9 cleavage.

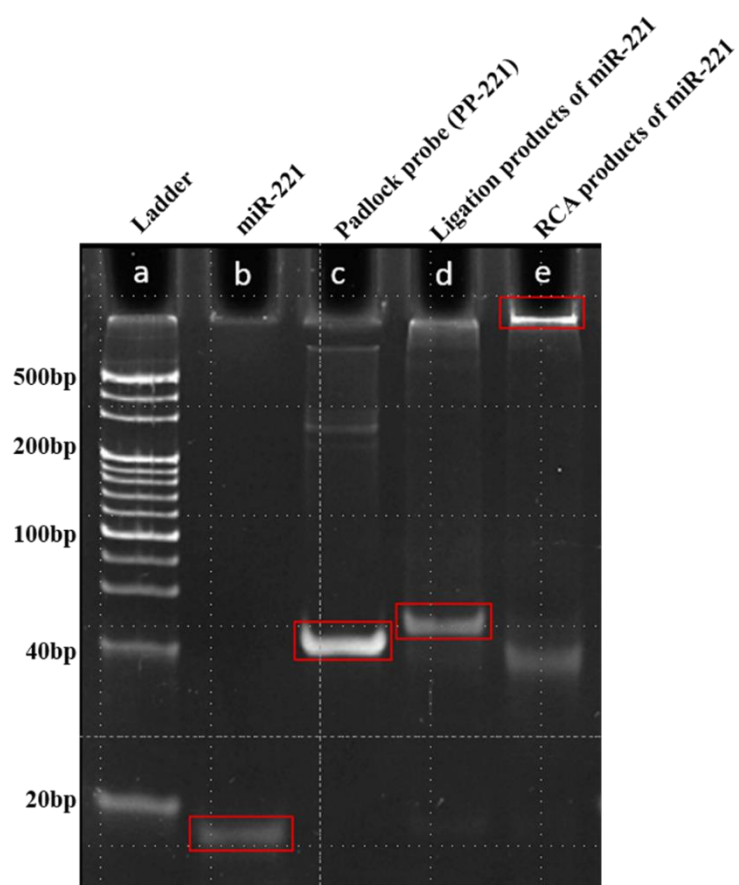


Figure S5. PAGE electrophoresis analysis of ladder (lane a), miR-221 (lane b), PP-221 (lane c), Ligation products of miR-221 (lane d), RCA products of miR-221 (lane e).

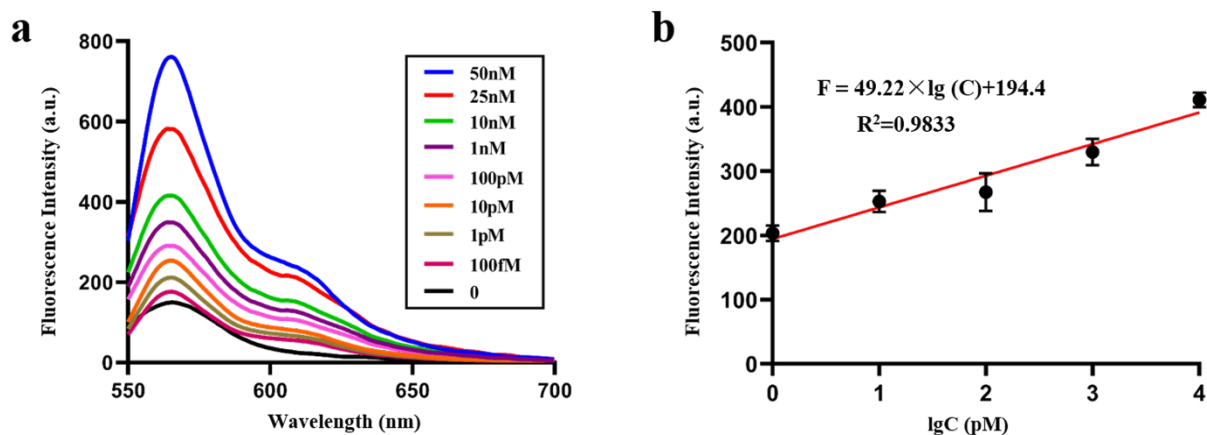


Figure S6. **a** Representative FI is well correlated with the concentration of miR-221 in DEPC water.

b The concentration change of miR-221 in DEPC water is linearly related to the FI through fitting curves, $F = 49.22 \times \lg(C) + 194.4$ ($R^2 = 0.9833$).

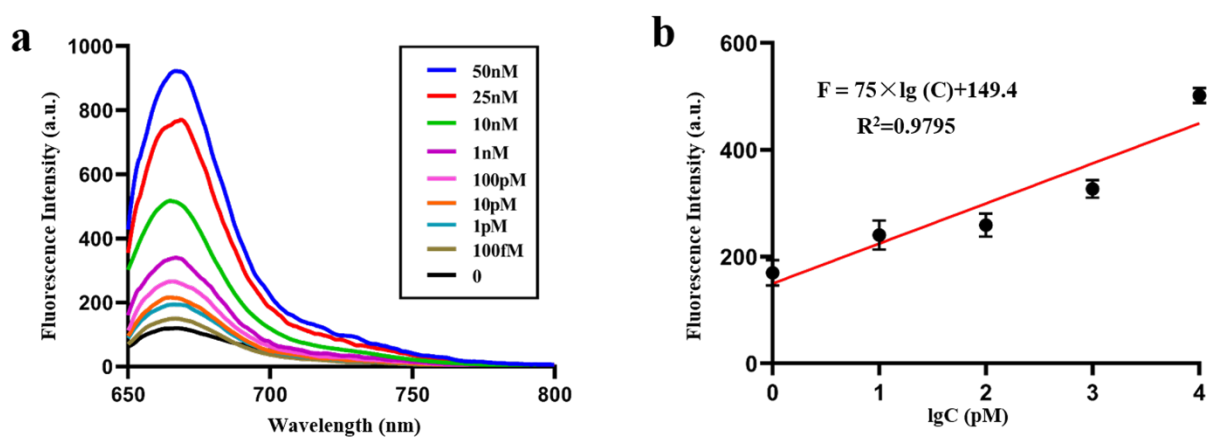


Figure S7. **a** Representative FI is well correlated with the concentration of miR-222 in DEPC water.

b The concentration change of miR-222 in DEPC water is linearly related to the FI through fitting curves, $F = 75 \times \lg(C) + 149.4$ ($R^2 = 0.9795$).

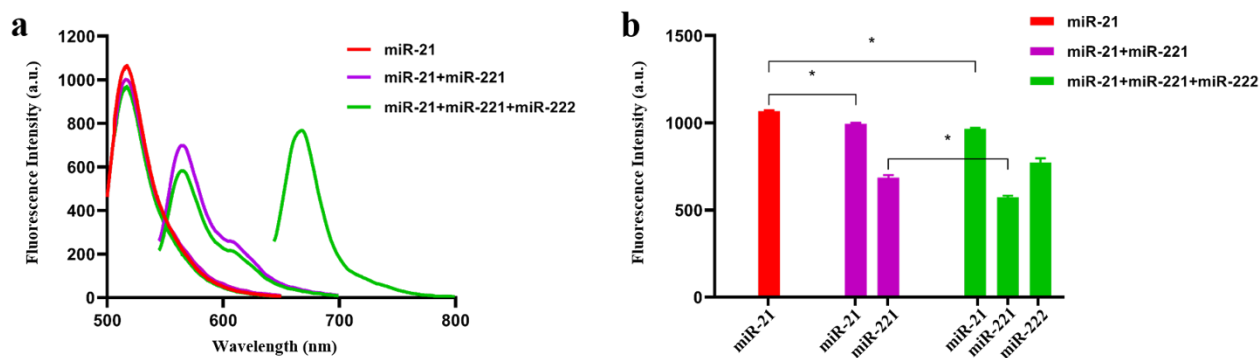


Figure S8. Representative interference experiments for miR-21 (50 nM) detection. **a** Fluorescence spectrum of different mixture. Red is miR-21 (50 nM) alone, pink is the mixture of miR-221 (50 nM) and miR-21 (50 nM), and green is the mixture of miR-21, miR-221, and miR-222 with a concentration of 50 nM. **b** Representative FI peak value of one target or multiple targets. *, $P > 0.05$.

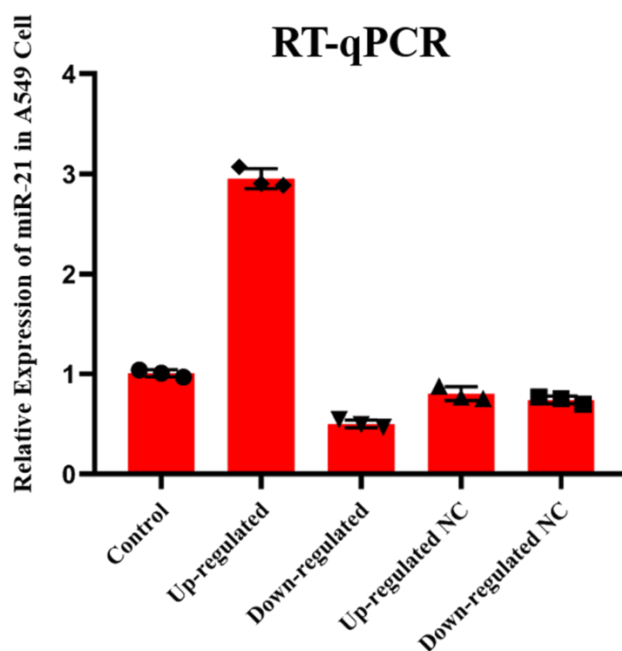


Figure S9. Cellular miR-21 determined by RT-qPCR. The relative expression of miR-21 in cell of up-regulated group was 2.94 times higher compared with the control group, and the down-regulated group was about 0.46 times of control group. Data were expressed as mean \pm standard deviations, $n=3$ sample replicates.

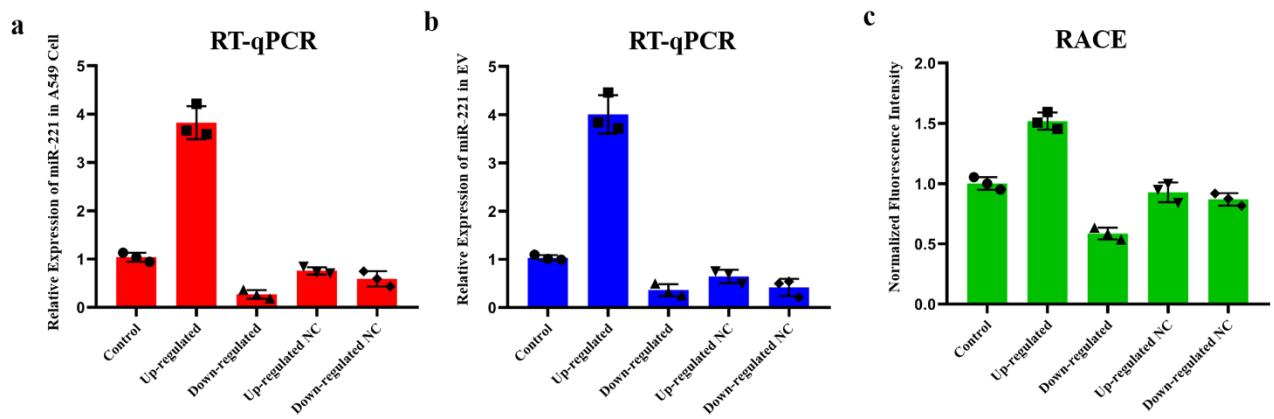


Figure S10. Methodological comparison between RT-qPCR and RACE in detecting miR-221. **a** miR-221 in cell detected by RT-qPCR. **b** miR-221 in EVs detected by RT-qPCR. **c** miR-221 in EVs detected by RACE. NC: negative control of regulated groups that are transfected invalid sequence into cells and does not affect the expression of miRNAs to verifying whether the regulated groups is successful or not. Data were expressed as mean \pm standard deviations, n=3 sample replicates.

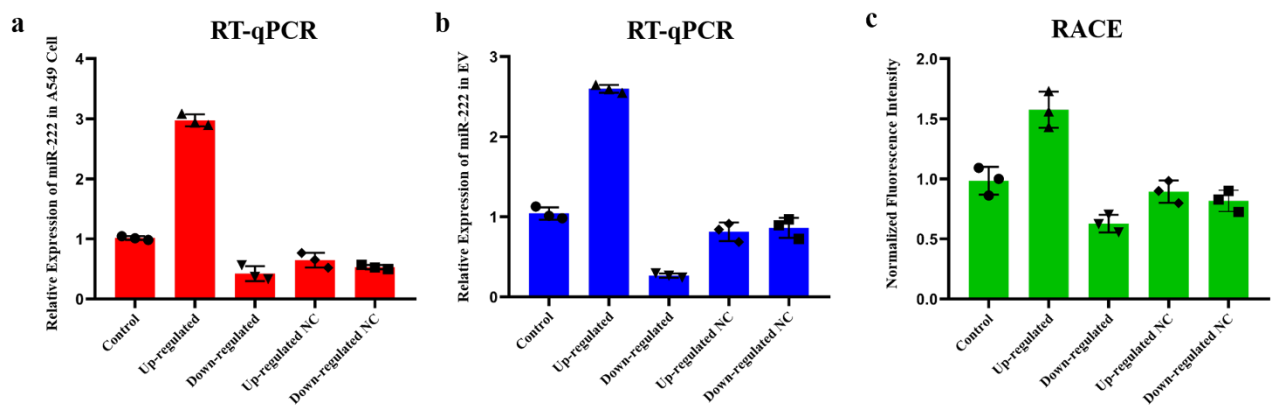


Figure S11. Methodological comparison between RT-qPCR and RACE in detecting miR-222. **a** miR-222 in cell detected by RT-qPCR. **b** miR-222 in EVs detected by RT-qPCR. **c** miR-222 in EVs detected by RACE. NC: negative control of regulated groups that are transfected invalid sequence into cells and does not affect the expression of miRNAs to verifying whether the regulated groups is successful or not. Data were expressed as mean \pm standard deviations, n=3 sample replicates.

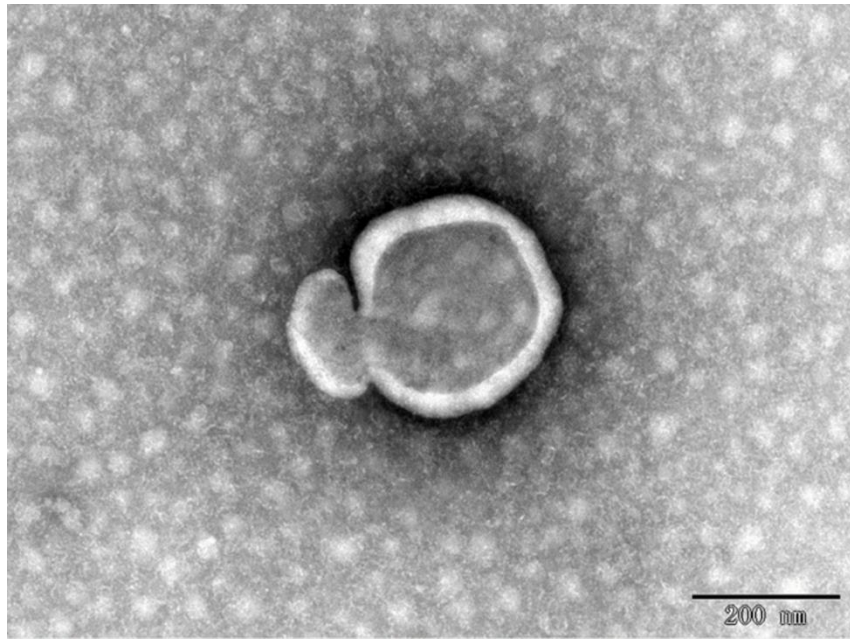


Figure S12. TEM image of the isolated extracellular vesicles from plasma. Scale bars: 200 nm.

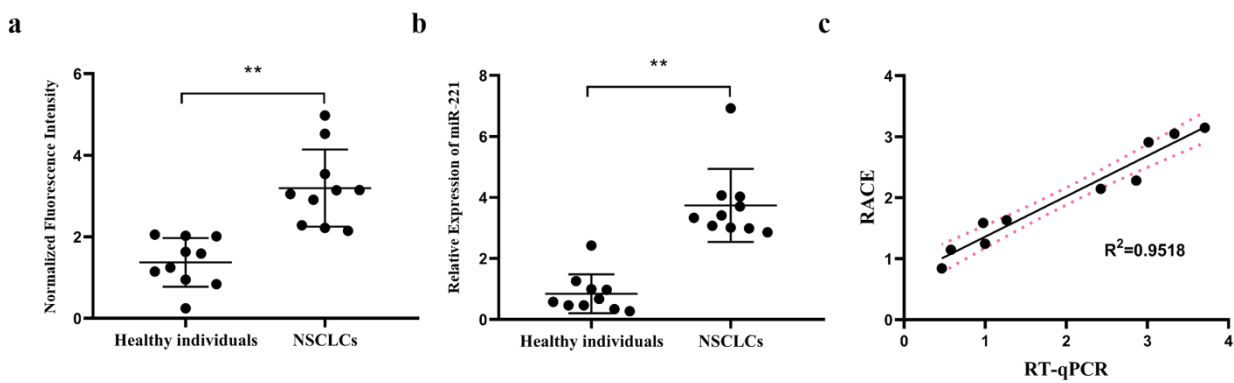


Figure S13. Plasma EV-derived miR-221 was detected between healthy individuals and NSCLCs patients. **a** Normalized fluorescence intensity of miR-221 in healthy individuals and NSCLCs patients by RACE, $\bar{x}_{\text{NSCLCs}}/\bar{x}_{\text{control}}=2.32$. **b** Relative expression of miR-221 in healthy individuals and NSCLCs patients by RT-qPCR, $\bar{x}_{\text{NSCLCs}}/\bar{x}_{\text{control}}=4.42$. **, $P<0.01$. **c** The fitting curves of regression analysis of RACE and RT-qPCR in detecting miR-221, $R^2=0.9518$, $P<0.0001$. Data were expressed as mean \pm standard deviations, $n=10$ sample replicates.

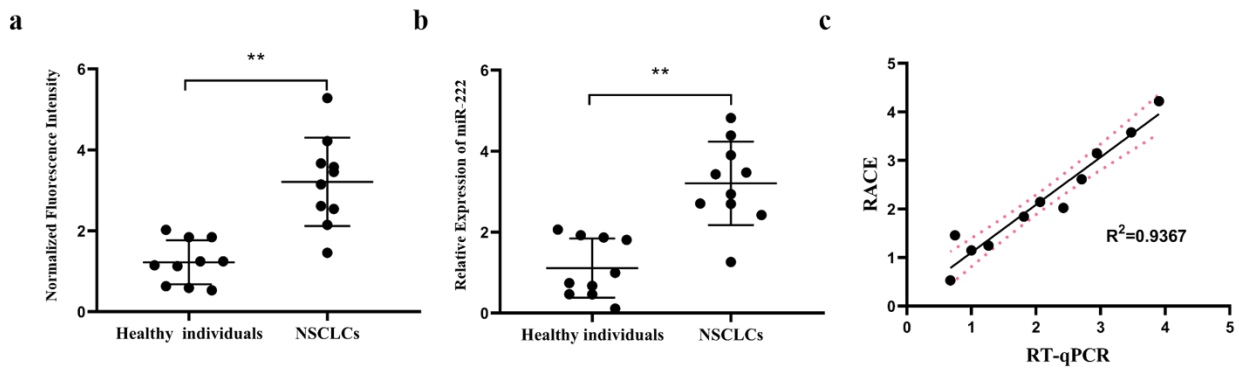


Figure S14. Plasma EV-derived miR-222 was detected between healthy individuals and NSCLCs patients. **a** Normalized fluorescence intensity of miR-222 in healthy individuals and NSCLCs patients by RACE, $\bar{x}_{\text{NSCLCs}} / \bar{x}_{\text{control}} = 2.32$. **b** Relative expression of miR-222 in healthy individuals and NSCLCs patients by RT-qPCR, $\bar{x}_{\text{NSCLCs}} / \bar{x}_{\text{control}} = 4.42$. **, $P < 0.01$. **c** The fitting curves of regression analysis of RACE and RT-qPCR in detecting miR-222, $R^2 = 0.9518$, $P < 0.0001$. Data were expressed as mean \pm standard deviations, $n = 10$ sample replicates.

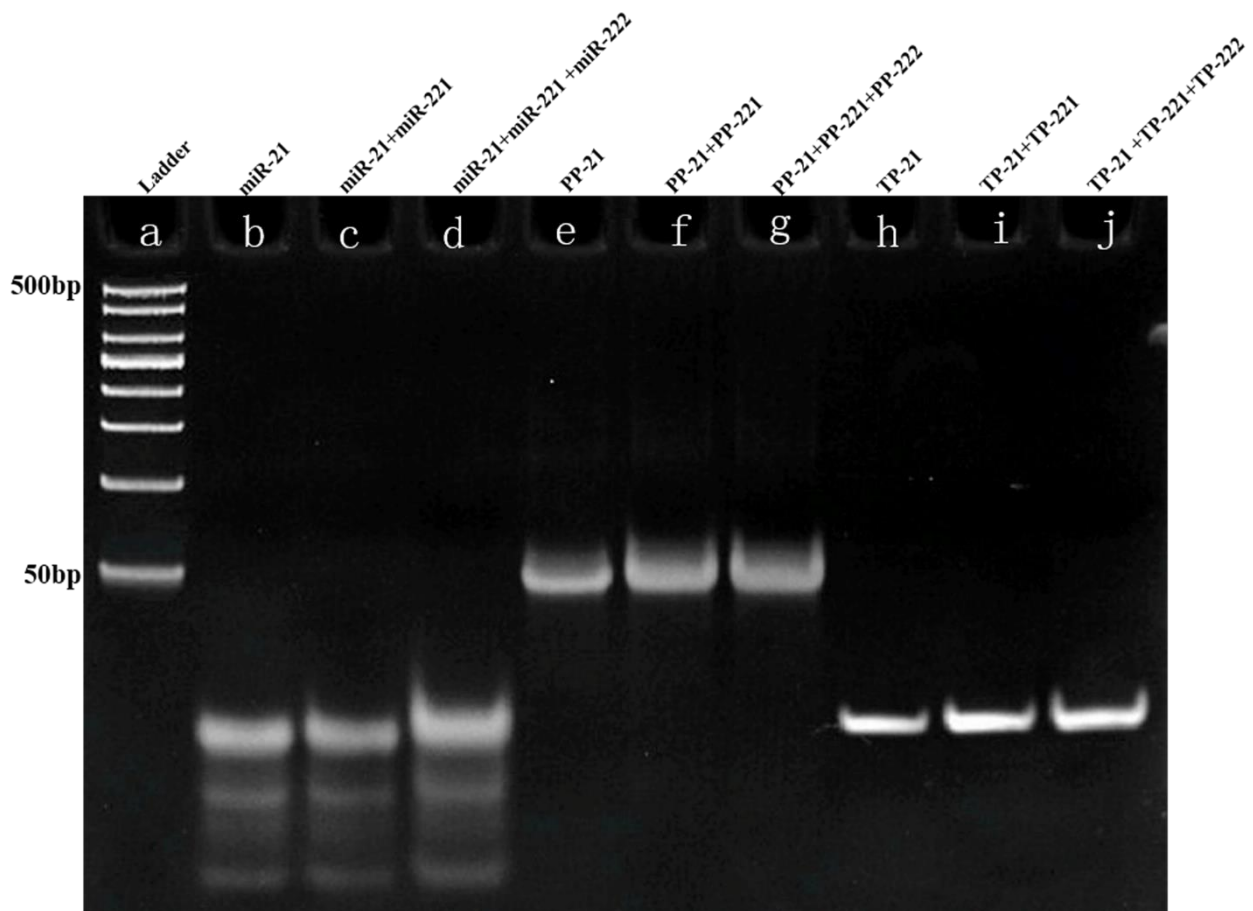


Figure S15. The PAGE electrophoresis analysis of multiple interferences.

Reference

- (1) Varallyay, E.; Burgyan, J.; Havelda, Z. *Nat. Protoc.* **2008**, *3*, 190-196.
- (2) Krepelkova, I.; Mrackova, T.; Izakova, J.; Dvorakova, B.; Chalupova, L.; Mikulik, R.; Slaby, O.; Bartos, M.; Ruzicka, V. *BioTechniques* **2019**, *66*, 277-284.
- (3) Lee, J. H.; Kim, J. A.; Kwon, M. H.; Kang, J. Y.; Rhee, W. J. *Biomaterials* **2015**, *54*, 116-125.
- (4) Lee, J. H.; Kim, J. A.; Jeong, S.; Rhee, W. J. *Biosens. Bioelectron.* **2016**, *86*, 202-210.